CT&F - Ciencia, Tecnología y Futuro - Vol. 6 Num. 4 Dec. 2016 Pag. 37 - 56

JOURNAL
CIENCIA, TECNOLOGÍA Y FUTURO

ISSN (Print) 0122-5383
ISSN (Online) 2382-4581

Journal of oil, gas and alternative energy sources

LITHOFACIES ANALYSIS AND DEPOSITIONAL ENVIRONMENT OF THE GALEMBO MEMBER OF LA LUNA FORMATION

ANALISIS DE LITOFACIES Y AMBIENTE DE DEPÓSITO DEL MIEMBRO GALEMBO DE LA FORMACIÓN LA LUNA

MODELOS DE GERAÇÃO DE HIDROCARBONETOS AO LONGO DO DEPRESSÃO BASAL DA ZONA DE SUBDUCÇÃO ANDINA NO NORTE DO EQUADOR E SUL DA COLÔMBIA

Efrain Casadiego-Quintero[1] and Carlos Alberto Ríos-Reyes*[1].

[1]Universidad Industrial de Santander, Bucaramanga, Santander, Colombia

e-mail: carios@uis.edu.co

(Received: Sep. 14, 2015; Accepted: Dec. 05, 2016)

ABSTRACT

The Cretaceous La Luna Formation at the Middle Magdalena Valley Basin is a classic shale-gas system in which the rock is the source, reservoir, and seal. It was deposited in a deep water marine environment with little oxygen in the sea floor. The Galembo Member comprises several lithofacies dominated by fine-grained (clay- to- silt-size) particles. Five lithofacies are recognized based on mineralogy, fabric, fossil content and texture: (1) nonlaminated to slight laminated foraminifera wackestones, (2) moderate to well-laminated highly fossiliferous claystones rich in organic matter; (3) claystones with fossiliferous carbonate concretions with pyrite; (4) nonlaminated siliceous and fossiliferous claystones; (5) ash falls.
Each facies contains abundant pyrite and phosphate. Carbonate concretions are also common.
The fossil content shows a predominantly deep marine paleoenvironment of deposition. Minor changes can generate variations in the relative proportion of terrigenous material, precipitation of organic matter and diagenetic alterations. Its deposition is estimated to have occurred over a 25- m.y. period, and despite the variations in sublithofacies, sedimentation style remained remarkably similar throughout this span of time.

Keywords: *Galembo Member, La Luna Formation, Shales, Lithofacies, Depositional environment.*

How to cite: Casadiego-Quintero, E., Ríos-Reyes, C. A. (2016). Lithofacies analysis and depositional environment of The Galembo member of La Luna Formation. *CT&F - Ciencia, Tecnología y Futuro*, 6(4), 37 - 56.

**To whom correspondence should be addressed*

RESUMEN

La Formación La Luna del Cretáceo en la Cuenca del Valle Medio del Magdalena es un sistema clásico de shale gas en el que la roca es fuente, reservorio y sello. Esta fue depositada en un ambiente marino de aguas profundas, con poca oxigenación en el fondo. El Miembro Galembo presenta litofacies dominadas por partículas (tamaño arcilla a limo) de grano fino. Cinco litofacies se reconocen según su mineralogía, fábrica, contenido fósil y textura: (1) wackestones con foraminíferos no laminados a ligeramente laminados, (2) arcillolitas muy fosilíferas y ricas en materia orgánica moderadamente a muy laminadas; (3) arcillolitas con concreciones de carbonato fosilíferas con pirita; (4) arcillolitas silíceas y fosilíferas no laminadas; (5) caídas de ceniza. Cada facies contiene abundante pirita y fosfato. Las concreciones de carbonato también son comunes. El contenido fósil revela un paleoambiente marino de deposición predominantemente profundo. Pequeños cambios pueden generar variaciones en la proporción relativa de material terrígeno, la precipitación de la materia orgánica y alteraciones diagenéticas. Su depositación se estima que se produjo sobre un periodo de 25-ma, y a pesar de las variaciones en sublitofacies, el estilo de sedimentación se mantuvo notablemente similar en todo este lapso de tiempo.

Palabras clave: *Miembro Galembo, Formación La Luna, Shales, Litofacies, Ambiente de depósito.*

RESUMO

A Formação La Luna del Cretáceo na Bacia do Vale Médio do Magdalena é um sistema clássico de shale gas onde a rocha é fonte, reservatório e selo. A formação ficou depositada em um ambiente marinho de águas profundas, com pouca oxigenação no fundo. O Membro Galembo apresenta litofacies dominadas por partículas (tamanho argila a limo) de grão fino. Cinco litofacies são reconhecidas segundo a sua minerologia, fábrica, conteúdo fóssil e textura: (1) wackestones com foraminíferos não laminados a levemente laminados, (2) argillites muito fossilificas e ricas em matéria orgânica moderadamente a muito laminadas; (3) argillites com concreções de carbonato fossilificas com pirita; (4) argillites silíceas e fossilificas não laminadas; (5) quedas de cinza. Cada facies contém abundante pirita e fosfato. As concreções de carbonato também são comuns. O conteúdo fóssil revela um paleoambiente marinho de deposição predominantemente profundo. Pequenas mudanças podem gerar variações na proporção relativa de material terrígeno, a precipitação da matéria orgânica e alterações digenéticas. Estima-se que o seu depósito aconteceu sob um período de 25-ma, e apesar das variações em sublitofacies, o estilo de sedimentação se manteve significativamente similar neste intervalo de tempo.

Palavras-chave: *Membro Galembo, Formação La Luna, Shales, Litofacies, Ambiente de depósito.*

1. INTRODUCTION

The history of the Earth has gone through several episodes. One of these episodes, that has enormous economic repercussions, took place during the mid-Cretaceous time (80–125 Ma) and led to deposition of organic carbon-rich sediments, informally known as black shales, over large regions of the ocean (Bralower and Lorente, 2003). According to Poulsen, Barron, Arthur, & Peterson, 2001, the marine record offers an attractive, yet incomplete, view of the mid-Cretaceous global ocean circulation. During periods of oceanic black shale deposition, deeper oceanic waters must have been suboxic to anoxic, atmospheric partial pressures of oxygen and nitrous oxides probably rose, and sea levels rose to a maximum of ca. 270 m (Russell and Paesler, 2003). Deposition of black shales resulted from several factors, including warm oceanic deep waters with low dissolved-oxygen contents, sluggish circulation in tectonically restricted basins, and elevated levels of marine productivity (e.g., Arthur, Schlanger, & Jenkyns, 1987; Erbacher, Huber, Norris, & Markey, 2001.; Russell and Paesler, 2003). Carbon derived from terrestrial plants is often abundantly represented in Mid-Cretaceous black shales (Bersezio, Erba, Gorza & Riva, 2002). However, recent research has shown that the volume of carbon locked up in Cretaceous-age sediments in continental-margin locations, such as Colombia (Mann and Stein, 1997; Villamil, 1999), far outweighs that contained in deep-sea settings, with marginal carbon-rich sediments being lithologically and geochemically more diverse and stratigraphically more variable than their open-ocean counter-parts (Bralower and Lorente, 2003). Since the production of conventional oil and gas drops in recent years, the focus of interest has been directed toward unconventional reservoirs (hydrocarbons in rocks of nanometric porosity and low permeability extracted with new developing methods as fracking. Gas shales are part of the unconventional gas reservoirs and were considered as viable economic resources after 70s when hydrocarbon price increased in the United States of America (Law and Curtis, 2002). For this reason, it has been very important to understand gas shales, where expulsion, migration and trapping occur in the source rock (Ross and Bustin, 2009). According to reports from the ANH (Agencia Nacional de Hidrocarburos) (2008), Colombia has oil reserves for about seven years, but the focus on unconventional reservoirs hopes to provide the country with new unlocked reserves. The potential is approximately 100 million barrels of equivalent oil, out of which 50% to accounts for natural gas. Crude oils in the Middle Magdalena Valley Basin (MMVB) of Colombia, which have accumulated in Tertiary fluvial-sand reservoirs, also have been generated, based on geochemical-correlation techniques such as stable-carbon-isotope ratios and geochemical fossil distributions in part, from the La Luna Formation of Cretaceous age (Zumberge, 1980). Although the MMVB has been widely explored for conventional reservoirs, still contains one of the most prolific plays of non-conventional resources, which have received considerable attention worldwide. The geological setting of the La Luna Shale play has been the object of several publications (e.g., Morales *et al*., 1958; Schamel, 1991; Montgomery, 1992). According to previous studies (e.g., Rangel *et al*., 2000b; Mayorga and Piamonte, 2015), the Galembo Member shows HI of ~495, average OI of 22, TOC of ~2-4%, S_2 of 12, kerogen II and T_{max} of ~433º, which compared with Vaca Muerta in Argentina and Barnett in the United States of America can be one of the members of the La Luna Formation with the higher potential of gas shale. According to Slatt (2011), apart from the geochemical characteristics, the lithological properties influence the fragility of the rock and subsequent fracturing, which is essential in the production of gas shale. The Galembo member is composed of black calcareous claystones interbedded with argillaceous limestones (Morales *et al*., 1958), with frequent thin layers of black chert (Ramon and Dzou, 1999) with numerous concretions inside, whereas other studies (e.g., Rangel, Parra, & Niño, 2000b; Ballesteros and Parra, 2012) describe interbedded limestones and phosphatic shales, revealing a depositional setting in shallow marine environment conditions during the Coniaciano to Santonian time (Morales *et al*., 1958; Naranjo, Duque, & Moreno, 2009). This study is intended to characterize the lithofacies of the upper part (the Galembo Member) of the La Luna Formation, in order to define its depositional setting.

2. GEOLOGICAL SETTING OF THE MMVB

The MMVB is a north-south trending intermontane basin located between the Eastern and Central cordilleras of Colombia (Figure 1), which has produced most of the oil and gas in Colombia with over 40 discovered conventional oil fields, sourced out of Tertiary sandstone reservoirs (Rodriguez, 2013). It

has been the focus of shale exploration leasing and drilling activities. Historically, the MMVB has been an important source for the conventional onshore production of hydrocarbons. Several papers about source rocks and petroleum systems have been published (e.g., Zumberge, 1984; Schamel, 1991; Ramon and Dzou, 1999; Rangel *et al*., 2000a; 2000b; Aguilera *et al*., 2009). Since the pioneering work of Garner (1926), several studies have been developed on the La Luna Formation (e.g., Hedberg and Sass, 1937; Hubach, 1957; Morales, 1958; Talukdar, Gallango, & Ruggiero, 1985; Ramon and Dzou, 1999; Rangel *et al*., 2000a, 2000b; Bralower and Lorente, 2003; Rey, Simo, & Lorente, 2004; Juliao, Suárez-Ruiz, Marquez, & Ruiz, 2015). It has long been considered to be the main hydrocarbon source rock in the MMVB by several authors (e.g., Zumberge, 1984; Rangel *et al*., 1996), as well as in other important basins such as the Maracaibo Basin of Venezuela (e.g., Hedberg and Sass, 1937; Young, Monaghan, & Schweisberger, 1977; Talukdar *et al*., 1985) and can be considered as a self-contained source and reservoir system and thus constitutes an unconventional shale play (Torres, 2013). The organic-rich Cretaceous La Luna Formation, which is similar to the one described in Venezuela (Zumberge, 1984), is the main source rock of the MMVB in Colombia (Zumberge, 1984; Govea and Aguilera, 1985; Perez-Tellez, 1994), and is emerging as one of the major gas plays of the region and is among the top worldwide shale gas systems. According to Torres (2013), this formation can be described as calcareous black shales and limestones, with high foraminifera content and calcareous and phosphate concretions; based on the facial analysis, the depositional environment is believed to be shallow marine, middle to outer shelf, in a transgressing sea. Morales (1958) subdivided the La Luna Formation into three members from base to top: Salada, Pujamana and Galembo. According to Zumberge (1984), the thickness of the formation varies from 150 to 600 m. The Salada Member consists of hard, black, thinly bedded, finely laminated, limy shales with some thin beds of black fine-grained limestones. It contains abundant planktonic foraminifera and radiolarian but lacks benthonic foraminifera. The occurrence of streaks and concretions of pyrite are characteristic of this member. The Pujamana Member is composed of gray to black, calcareous, thin- bedded shale. The Galembo Member consists of thin bedded, black, calcareous shale with interbeds of thin argillaceous limestones (e.g., Morales *et al*., 1958; Ramon and Dzou, 1999; Casadiego, 2014). Frequent thin beds of blue-black cherts occur, with numerous ammonite- bearing concretions being found in this member (e.g., Naranjo *et al*, 2009; Casadiego, 2014). The three members of the La Luna Formation contain variable carbonate contents: The Galembo Member generally contains minor-to-trace amounts of carbonate (2,4%), in contrast, the Pujamana and Salada members are carbonate-rich (43,2% and 40,4%), respectively (Zumberge, 1984). TOC values in the Pujamana and Salada members average approximately 3.5 wt% and 4.5 wt%, respectively (Zumberge, 1984), whereas Total Organic Carbon (TOC) values in the Galembo Member reach 2.4% (Rangel, 2000b). According to Torres, Slatt, Philp, O´Brien, & Rodriguez, (2015). the La Luna Formation was deposited under dysoxic/anoxic episodic periods during major transgressive-regressive cycle and therefore major third order stratigraphic cycles can be recognized, including transgressive systems tract (TST), highstand systems tract (HST) and transgressive surface of erosion (TSE), as follows: the base of the lower Salada member: TST-HST-TST; TST at the Salada member top; Pujamana member deposition was interpreted as a HST (second sequence boundary and TSE); Pujamana-Galembo boundary corresponds to deposition of TST; Galembo member occurred during a TST phase towards HST at the La Luna Formation top. The Galembo member, which is the focus of this study, has been studied in several aspects by different authors (e.g., Maughan *et al*., 1979; Ballesteros and Parra, 2012; Torres, 2013; Torres *et al*., 2012, 2015; Pacheco-Sintura *et al*., 2015).

3. FIELD SAMPLING AND ANALYTICAL METHODS

The investigated samples come from the Cretaceous La Luna Formation, particularly from the Galembo Member, and were collected from several outcrops along the eastern flank of the Nuevo Mundo Syncline in the MMVB approximately 20 km west of Bucaramanga, Colombia. A stratigraphic column of about 50 m of thickness was described in the section of the Aguablanca Stream. It was accompanied by a systematic sampling. The classification of Folk (1974) for terrigenous rocks and Dunham (1962) for allochemical/orthochemical rocks were adopted in the classification. The geochemical data were obtained on the basis of the following analytical data: % (TOC) and Rock–Eval Pyrolysis. Rock samples were ground to <100 mesh with subsequent carbonate

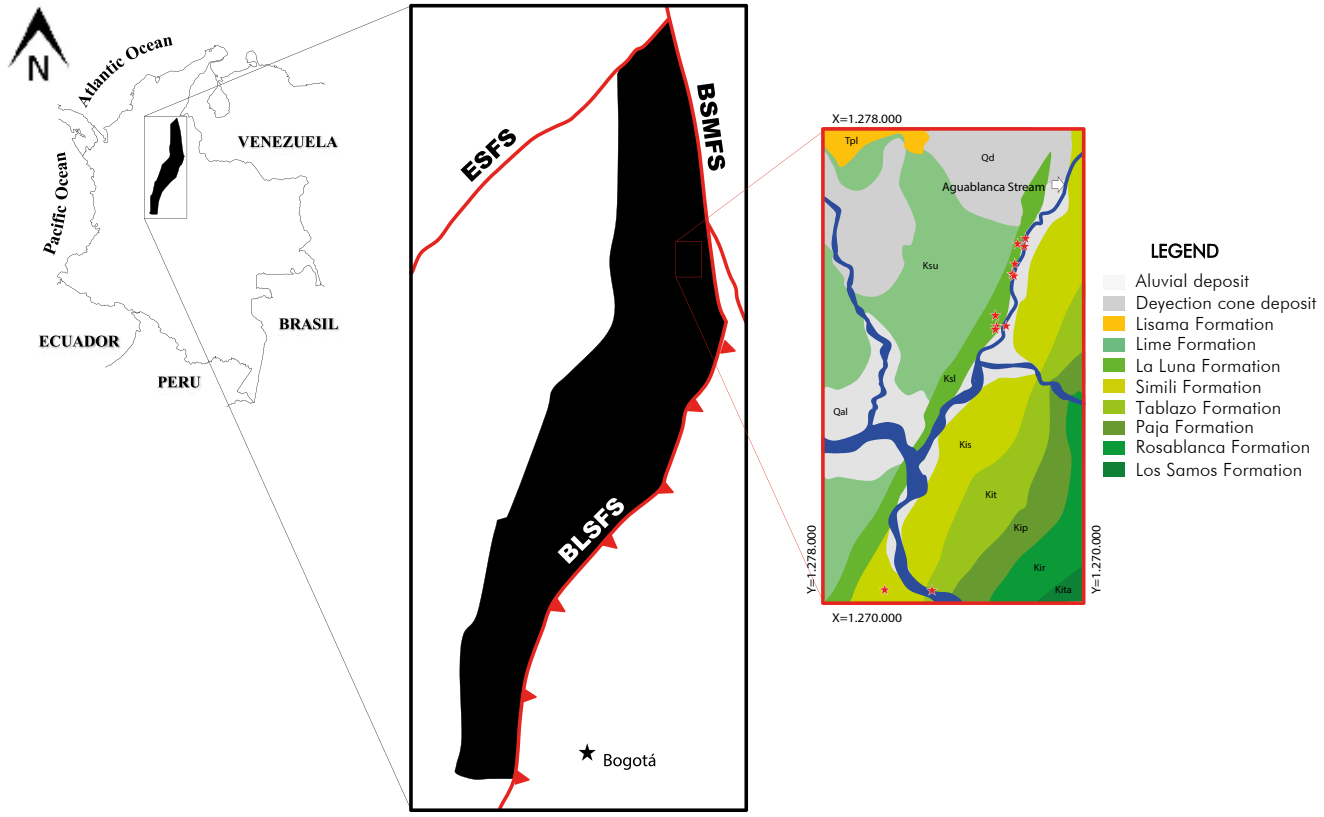

Figure 1. Left, location of the MMVB (black polygon) in Colombia. Figure notations: the Bituima and La Salina fault systems (BSFS); the Espiritu Santo fault system (ESFS); the Bucaramanga-Santa Marta fault system (BSMF) (adapted and modified from ANH, 2008). Sampling localions is indicated by red stars.

dissolution with HCl and organic-carbon combustion using a LECO WR 112 Carbon Analyzer in order to determine the total organic carbon (TOC). Taking into account parameters of geochemical interpretation, a "cut off" where only samples with TOC greater than or equal to 0.8% were considered for pyrolysis. Rock–Eval Pyrolysis is generally used to identify organic matter type and maturity level (e.g., Espitalié, Deroo, & Marquis, 1986.; Nuñez-Betelu and Baceta, 1994; Abdel-Rahman, 2013). This was performed using 100 mg of ground/powdered rock, and a Rock-Eval 6 device. Mineralogy analys were performed by collecting X-ray powder diffraction (XRPD) patterns. Samples were milled in an agate mortar and then mounted on a sample holder of Separar polymethyl methacrylate (PMMA) through the filling front technique. The XRPD pattern of garnet was recorded by X-ray diffraction using a BRUKER D8 ADVANCE diffractometer operating in Da Vinci geometry and equipped with an X-ray tube (Cu-Kα1 radiation: λ = 1.5406 Å, 40 kV and 30 mA), a 1- dimensional LynxEye detector (with aperture angle of 2.93o), a divergent slit of 0.6 mm, two soller axials (primary and secondary) of 2.5º and a nickel filter. Data collection was carried out in the 2θ range of 12-80°, with a step size of 0.01526° (2θ) and counting time of 1 s/step. Phase identification was performed using the crystallographic database Powder Diffraction File (PDF- 2) from the International Centre for Diffraction Data (ICDD) and the program Crystallographica Search-Match. The unit-cell constants, atomic positions, factors of peak broadening and phase concentrations were refined and calculated by using the MDI RIQAS program based on the Rietveld method. Twenty-nine thin sections were prepared for petrographic analyses from offcuts of the rock samples with the plane of the section normal to the macroscopic lamination. All samples were impregnated with epoxic resin and stained for carbonates and feldspars in order to recognize the porosity. Thin sections were point counted (300 grains per sample) using the Gazzi-Dickinson method (Ingersoll *et al.*, 1984). Petrographic analysis was performed using a trinocular Nikon (Labophot2-POL) transmitted light microscope equipped with an Olympus DP71 camera for image acquisition. Mineral abbreviations are retrieved

from Kretz (1983). More detailed analyses followed by means of environmental scanning electron microscopy (ESEM) using a FEI QUANTA FEG 650 instrument, under the following analytical conditions: magnification = 800-60000x, WD = 5.6-14.0 mm, HV = 10.0-20.0 kV, signal = ETD/Z CONT, detector = SE/BSED. Operational mode was mainly using secondary electrons (SE), although back scattered electrons (BSE), were also useful where contrasts in grey level in the images correspond to contrasts in atomic number and therefore chemical composition of the analyzed area. Particular areas of interest were analyzed to retrieve the chemical composition of the region via energy dispersive X-ray spectroscopy (EDS). EDS Detector EDAX APOLO X with resolution of 126.1 eV (in. Mn Kα).

4. RESULTS AND DISCUSSION

The Galembo Member interval of the La Luna Formation comprises a variety of lithofacies, which, with the exception of ash falls, are dominated by fine-grained (clay- to- silt-size) sediments. In this study, we recognize five general lithofacies in the Aguablanca section on the basis of mineralogy, fabric, fossil content and texture: (1) nonlaminated to slight laminated foraminifera wackestones, (2) highly fossiliferous moderate to well-laminated claystones rich in organic matter; (3) claystones with fossiliferous carbonate concretions with pyrite; (4) nonlaminated siliceous and fossiliferous claystones; (5) ash falls. These lithofacies will be discussed briefly in the sections below. The Galembo Member facies were defined from descriptions of outcrops in the Aguablanca section. General aspects of them are illustrated in Figure 2.

5. MINERALOGY AND LITHOLOGY

Thin-section, scanning electron microscopy and X-ray diffraction analysis (Figure 3) show that the Galembo Member interval of the La Luna Formation comprises several lithofacies. A ternary diagram of the Galembo Member mineralogical constituents show that the analyzed samples are composed mainly of allochemical, orthochemical and terrigenous minerals in different proportions with abundant proportions of carbonate planktonic foraminifera and other pelagic organisms, suggesting deposition in moderately deep water with restricted bottom circulation. The rocks of the Galembo Member are within the range of claystones. The mineral composition was determined under the transmitted light microscope, which was compared with

Figure 2. General outcrop features of the Galembo Member (La Luna Formation) in the Aguablanca section. Nonlaminated to slight laminated Wackestone (Ws), Claystone (Cs), Claystone fossiliferous (CsSi), Well-laminated, Claystone rich in organic matter (CsOm) and Carbonate Concretions (red arrow).

data from X-ray diffraction. The carbonate material is mainly rhombohedral dolomite, micrite, foraminifera, calcareous sponge spicules, bioclastic limestones and calcareous cement. The siliceous material includes sponge spicules, bioclasts filled by microcrystalline silica and chert, quartz and chert grains, siliceous matrix and cement. Other accessory minerals (feldspar, pyrite, zircon, opaque minerals and phosphates) comprising less than 3% of the rock were observed.

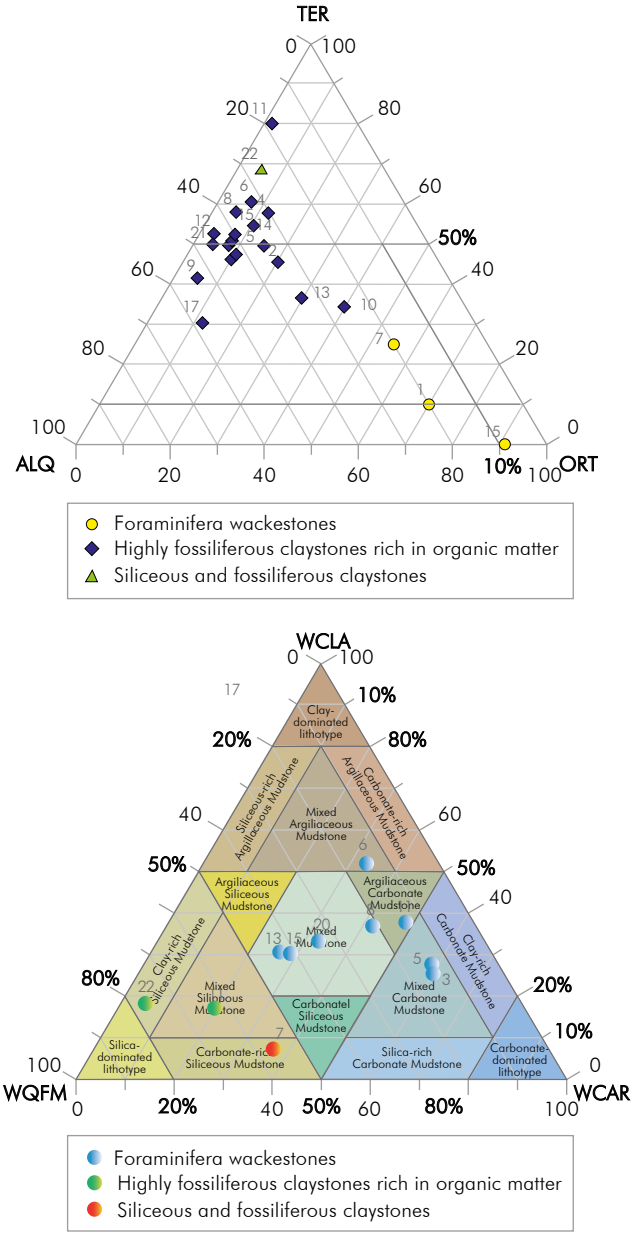

Figure 3. Ternary diagram of the mineralogical compositions of the Galembo Member (La Luna Formation), showing the distribution of the analyzed samples in the Aguablanca section.

6. LITHOFACIES

The Galembo Member contains five major lithofacies, which are discussed briefly in the sections below, according to the workflow followed in this study (Figure 4). They collectively show that the upper and lower part are composed dominantly of nonlaminated and slight-laminated foraminifera wackestones, moderate to well-laminated highly fossiliferous claystones rich in organic matter (sometimes with fossiliferous carbonate concretions with pyrite), and nonlaminated siliceous and fossiliferous claystones, with interlayered thin layers of ash falls. Casadiego (2014) recognized the following lithofacies in the Aguablanca section (Figure 5): (1) nonlaminated to slight laminated foraminifera wackestones, (2) highly fossiliferous moderate to well-laminated claystones rich in organic matter; (3) claystones with fossiliferous carbonate concretions with pyrite; (4) nonlaminated siliceous and fossiliferous claystones; (5) ash falls.

Nonlaminated to slight laminated foraminifera wackestones

This lithofacies represent the 35% of the Galembo Member interval in the Aguablanca section, although these rocks are highly variable in character. It shows net irregular contact with highly fossiliferous claystones rich in organic matter (Figure 6a) and contains intercalations of claystones with fossiliferous carbonate concretions with pyrite and ash falls. Vertical changes from one lithofacies to another can be sharp or gradational. Fabric ranges from nonlaminated to slight laminated. Nonlaminated rocks are not affected by bioturbation (Figure 6b). Stylolites and organic matter are commonly observed (Figures 6c y 6d). These rocks are mainly medium dark gray in color, although thin layers with higher content of fossils display a light gray color. On the other hand, fragments of white broken shells obliquely arranged are embedded in the matrix. Stylolites and agglomerates of organic matter were observed. It is mostly compossed of orthochemicals and impure allochemicals. The lamination decreases with increasing the carbonate content of the rock. It consists of a calcareous mineralogy including microsparite (52-78 wt%), and traces of micrite (3 wt%) and pseudosparite (3 wt%). Clay minerals are in the range of 6-8 wt%; silica mineralogy from 18 to 17 wt%; and calcareous mineralogy varies from 73 to 74 wt%. This occurs in most of the section, but it

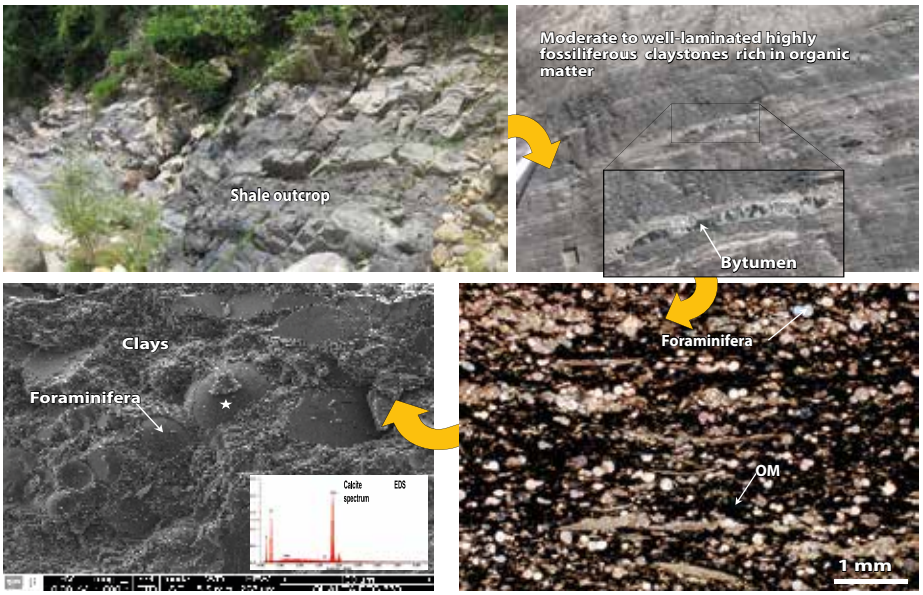

Figure 4. Multiscale workflow to characterize the Galembo Member (La Luna Formation) in the Aguablanca section.

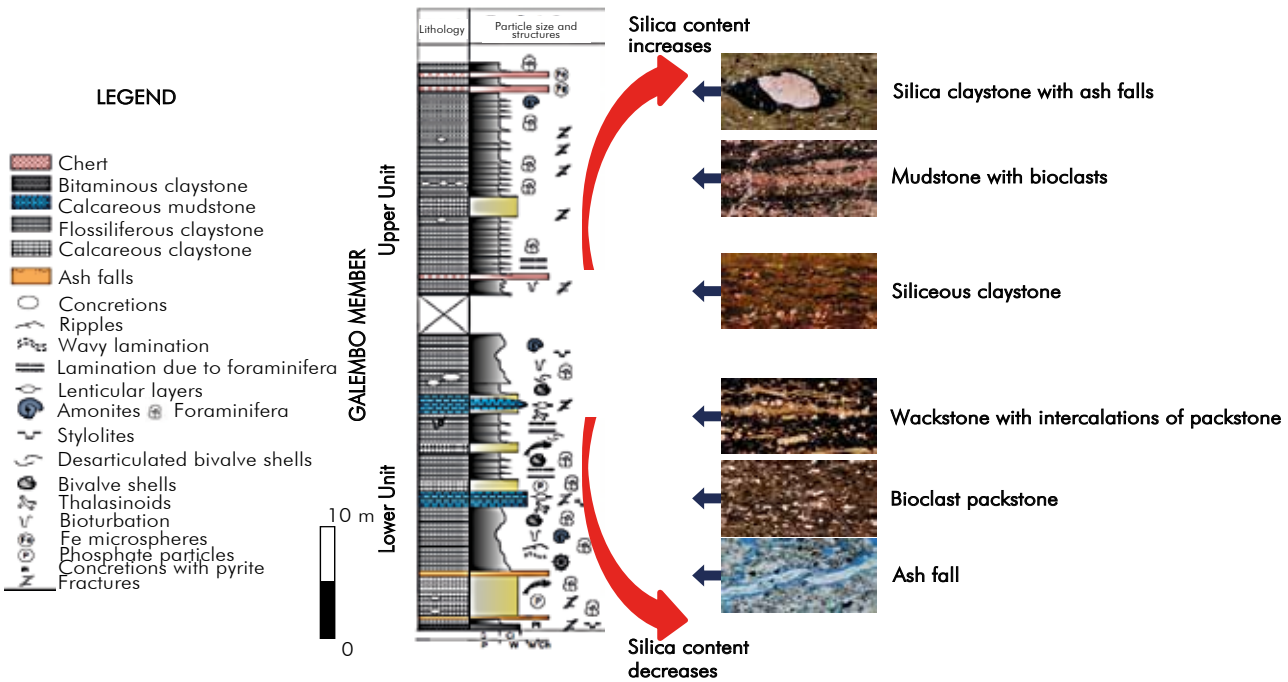

Figure 5. Generalized stratigraphic column of the Galembo Member (La Luna Formation) in the Aguablanca section, showing the sequence of microfacies.

is primarily seen at the base of thicker section. This lithofacies shows a continuous irregular basal contact. It is rich in foraminifera, with minor amount of spicules of echinoderms, bivalves and bioclasts replaced by calcite and pyrite; the organic matter is found in clusters embedded in calcareous cement. Most foraminifera appear with its longest axis, which is due to the cross section cut. Foraminifera are agglutinated together by forming floccules in a carbonate mud, which in most cases suffered diagenesis and aggrading neomorphism (Flügel, 2010) during the process of recrystallization (microsparite and pseudosparite). This facies represents a change in depositional environment shallower than that for highly fossiliferous claystones rich in organic matter and siliceous and fossiliferous claystones, with greater abundance of foraminifera and calcite of authigenic origin in the matrix. The main petrographic features of the nonlaminated to slight laminated foraminifera wackestones are illustrated in Figures 7 and 8.

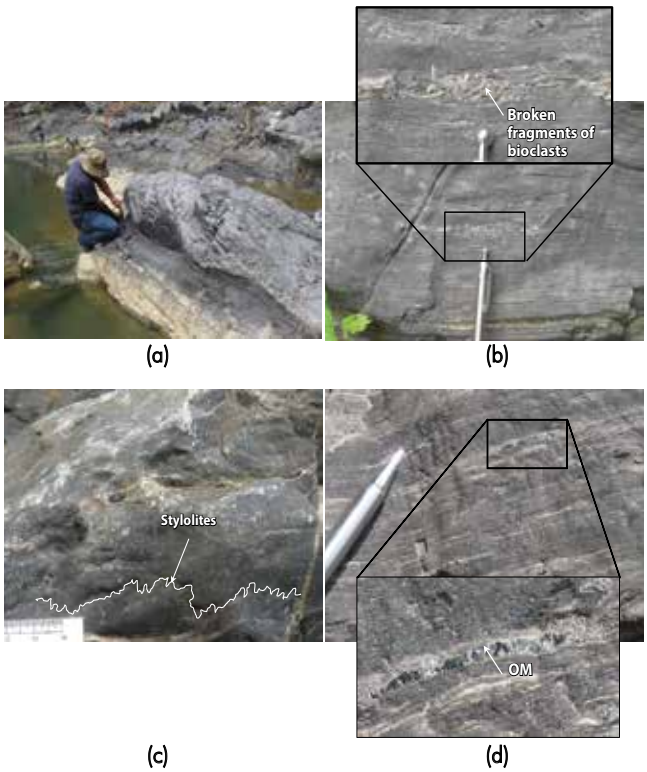

Figure 6. Photographs at outcrop scale of the nonlaminated to slight laminated foraminifera wackestones: a) Undulating contact to the bottom of this lithofacies. b) Broken fragments of bioclasts obliquely organized. a)-d) Foraminifera wackestones. Note the massive c) to slightly laminar d) structure, and also the occurrence of stylolites and organic matter.

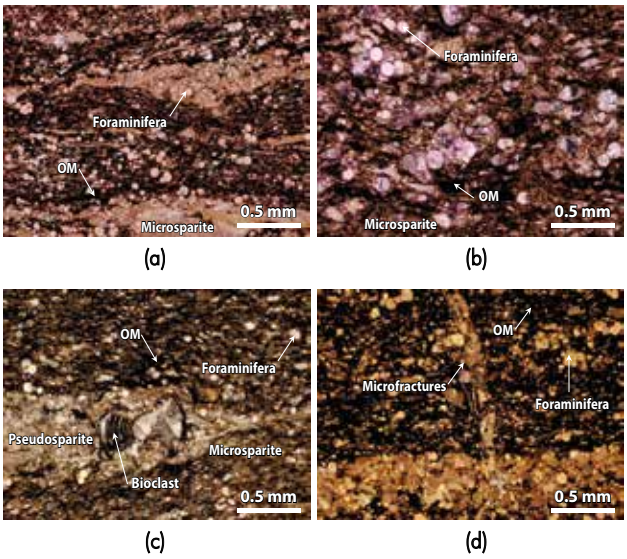

Figure 7. Photomicrographs in crossed polarized light of the nonlaminated to slight laminated foraminifera wackestones. a)-b) OM-rich layers interbedded into carbonate rich layers, which contain numerous dispersed foraminifera. c) OM-rich microsparite matrix where numerous foraminifera and scarce bioclasts occurs. d) OM-rich matrix, which shows numerous foraminifera and has been cross cut by several calcite veinlets that filled microfractures. OM, organic matter.

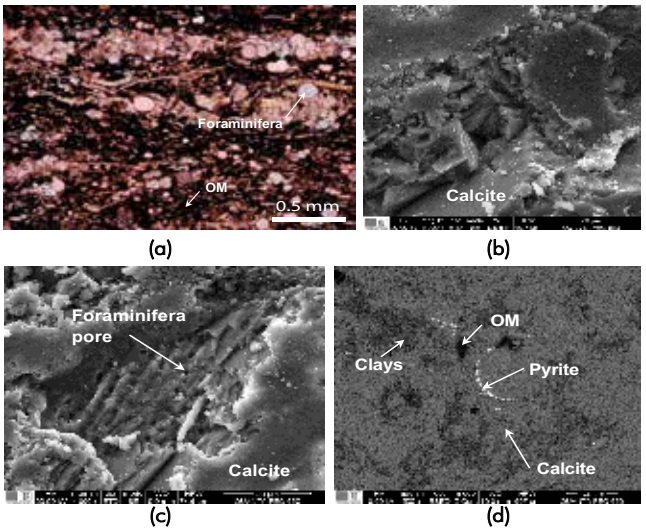

Figure 8. a) Photomicrograph in crossed polarized light of the nonlaminated to slight laminated foraminifera wackestones, showing OM-rich layers interbedded into carbonate rich layers, which contain numerous dispersed foraminifera. b)-c) Secondary electron (SE) SEM images of the occurrence of calcite and porosity associated toassociated with bioclasts (foraminifera), respectively. Backscattered electron (BSE) SEM image of the occurrence of pyrite and OM in a carbonate clay mineralogy. OM, organic matter.

Moderate to well-laminated highly fossiliferous claystones rich in organic matter

This is the most predominant lithofacies in the Aguablanca section (64%). This lithofacies is interlayered with foraminifera wackestones to the base of the section and siliceous and fossiliferous claystones to the top of the Aguablanca section (Figure 9). Its average layer thickness (0.3 to 4 m) tends to increase towards the top of the section. Most of all contacts with overlying and underlying siliceous and fossiliferous claystones are straight and sharp. Fabric ranges from nonlaminated to slight laminated to the bottom and lenticular to flaser laminated and laminar to massive structure towards the top. Ripple marks and laminar structures formed by the intercalation of fragments of bioclasts and clays. These rocks display a dark to middle gray color, and are composed mainly of clay and carbonate mineralogy with organic matter that is commonly observed in the matrix. Carbonate (calcite) is forming flocules in the matrix and filling foraminifera and developing discontinuous laminations. They also contain trace to minor amounts (7 wt%) of clay mineralogy, 36-73 wt% of carbonate mineralogy (represented mostly by foraminifera, fragments gastropods and bioclasts) and less than 9 wt% of clay mineralogy. Common biogenic components are foraminifera binders (0-40 wt%) and undifferentiated bioclasts (26 wt%). The few fragments

of shells and undifferentiated bioclasts are calcareous and show evidence of deformation and breakage during compaction. These rocks, which are characterized by a calcite-rich hemipelagic sedimentation with low nanofossil preservation, locally show some coccoliths and fragments of broken spicules. Pyrite appears in several forms. The most common are small framboids generally less than 10 mm in diameter and dispersed in the samples; most falling into the 1–2-mm range. Fine-grained framboids are commonly aggregated into larger masses. The fabric of these rocks show floccules of illite, which according to Schieber, Southard, & Thaisen, (2007) can be in contact face-to-face in hemipelagic seawater columns and edge-to-edge due to the electrostatic attraction. Silica is in the clay-size matrix and microcrystalline quartz lenses, which are of authigenic origin. The siliceous matrix component is evidenced by the moderate to high percentages reported by XRD analysis in whole rock ranging from 33 to 53 wt%. Terrigenous quartz greater than or equal to silt-size was not observed, so it follows that silica reported by XRD is part of the matrix (<4μm). This suggests that the higher the silica component the lower the carbonate and clay components. Claystones in the top of the section show bitumen filling fractures and some foraminifera. Accessory and trace minerals include phosphates, barite and apatite. SEM analysis reveals a siliceous composition with clay minerals (mainly illite floccules) developing flakes of irregular edges without preferential orientation and with face-to-face contact. Fabric is slightly planar and relatively open. The main petrographic features of the moderate to well-laminated highly fossiliferous claystones rich in organic matter are illustrated in Figures 10 and 11.

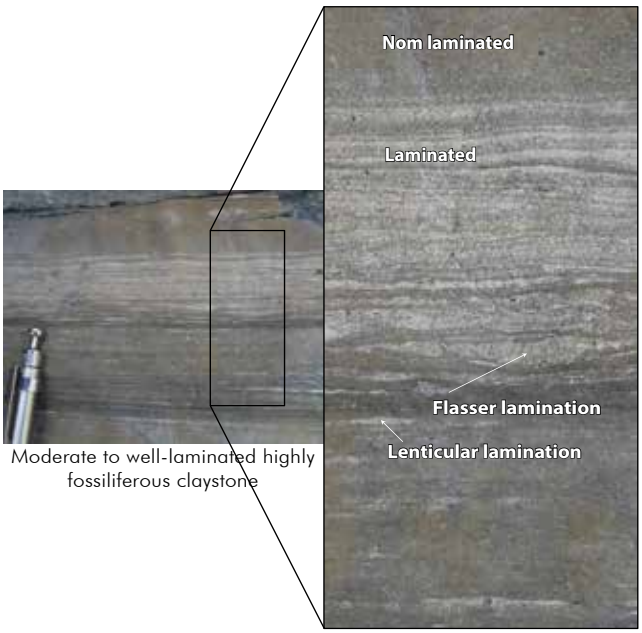

Figure 9. Photographs at outcrop scale of the moderate to well-laminated highly fossiliferous claystones rich in organic matter. Note the varying structural features: non laminated, lenticular and flasser structures.

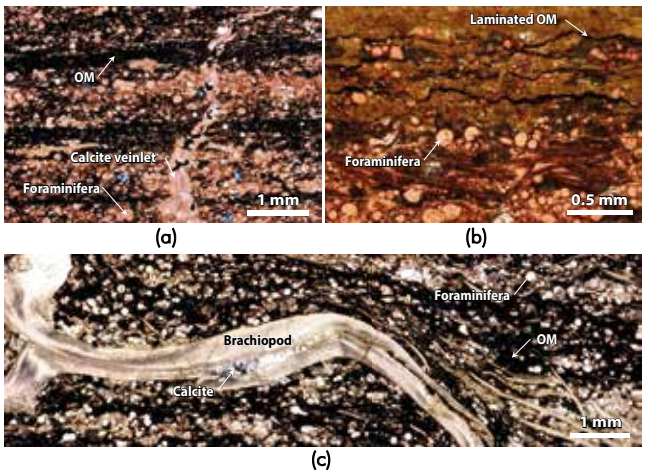

Figure 10. Photomicrographs in crossed polarized light of the moderate to well-laminated highly fossiliferous claystones rich in organic matter. a) OM-rich layers interbedded into carbonate rich layers, which contain numerous foraminifera. Note the occurrence of a calcite veinlet cross cutting the sedimentary structure. b) Slight deformed lamination, where laminated OM is interlayered into clay (and foraminifera) layers. c) Abundant OM in the matrix, where numerous spicules and a large brachiopod shell are observed. Note also the occurrence of foraminifera in calcite-rich layers. OM, organic matter.

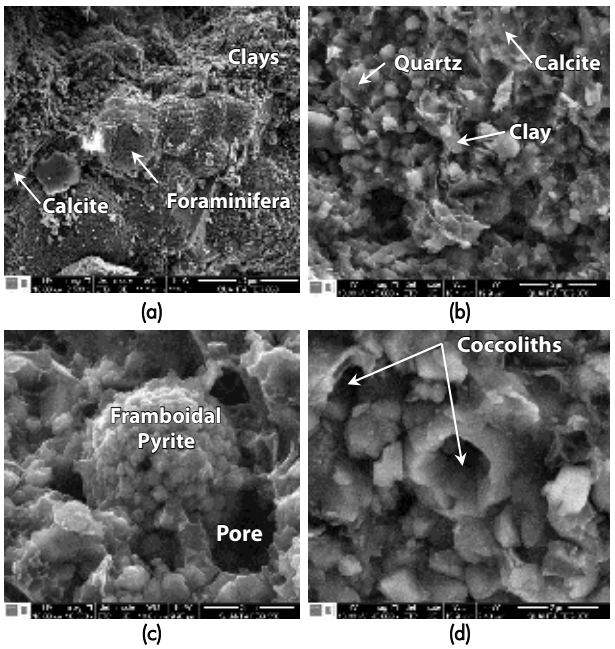

Figure 11. Secondary electron (SE) SEM images of main morphological features of the moderate to well-laminated highly fossiliferous claystones rich in organic matter. a) Foraminifera surrounded by a matrix dominated by a calcareous clay mineralogy. b) Main rock forking minerals, quartz, calcite and clay, developing a characteristic porosity. c) Framboidal Pyrite. Note the occurrence of interparticle pores. d) Porosity associated withto the occurrence of coccoliths.

Claystones with fossiliferous carbonate concretions with pyrite

This lithofacies constitutes 5% of the Aguablanca section. It is characterized by the occurrence of fossiliferous concretions with pyrite, with numerous subrounded very light gray to medium light gray carbonate concretions up to 30 cm in thickness formed in a state of early diagenesis due to early burial. Most concretions contain fossils such as bivalves and ammonites and pyrite (Figure 12). It also consists of dark grey claystones interlayered with fossiliferous claystones rich in organic matter. It shows irregular contact with the underlying and overlying layers, although it shows a net contact with the highly fossiliferous claystones rich in organic matter. Fabric is laminated. It consists entirely of microsparite and pseudosparite. Fragments of bioclasts filled by sparite were observed inside concretions. It shows a predominantly calcareous composition, with a few crystals of pyrite and organic matter. The main petrographic features of the claystones with fossiliferous carbonate concretions with pyrite are illustrated in Figure 13.

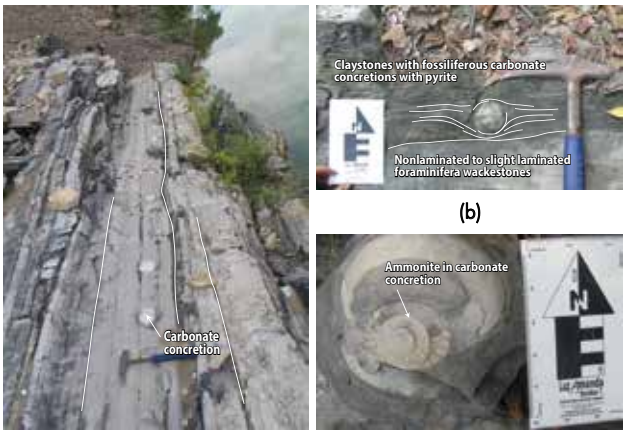

Figure 12. Photographs at outcrop scale of a) the claystones with fossiliferous carbonate concretions with pyrite. b) A concretion within claystone layer deformed by concretion compaction and overgrowth, in underlying contact with layers of foraminifera wackestones and highly fossiliferous claystones rich in organic matter. c) Ammonite in carbonate concretion.

Nonlaminated siliceous and fossiliferous claystones

It represents the 1% of the Aguablanca section and is characterized by the appearance of microcrystalline silica, moderate content of foraminifera and massive sedimentary structure. Reaction with acid attack is very low. These rocks show a grayish black to dark gray color, developing layers up to 15 cm in thickness, and are scarcely distributed mainly at the top of the section, particularly interlayered into highly fossiliferous claystones rich in organic matter, developing irregular and net contacts (Figure 14). The rocks of this lithofacies are mostly composed of clay minerals and foraminifera replaced by microcrystalline quartz. The matrix (65 wt%) is blackish brown and composed of indistinguishable minerals at petrographic level. According to the XRD analysis, the clay content is 27 wt%. The silica content (72 wt%) is supported by SEM and XRD analysis. Clay-rich sheets are undulous due to compaction around bioclasts (planktonic foraminifera and bioturbation). It is emphasized that authigenic microcrystalline silica is associated with silica floccules, which to a certain extent are characteristic of this lithofacies. This is quantified in the microcrystalline quartz reported in the clay fraction (< 2μm) XRD analysis (relative wt%), with the higher silica values being reported in all analyzed samples. The SEM analysis also reveals a siliceous matrix, euhedral calcite crystals, undifferentiated rounded siliceous bioclasts, and Fe-bearing bioclasts. The main

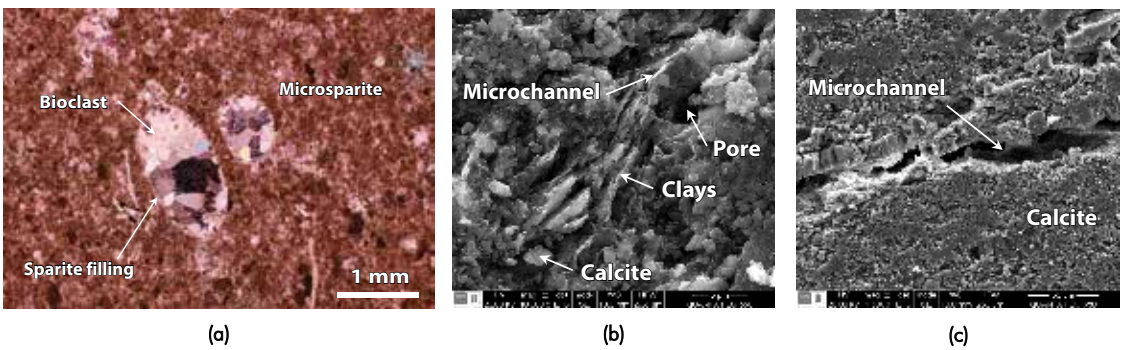

Figure 13. a) Photomicrograph in crossed polarized light of the claystones with fossiliferous carbonate concretions with pyrite, showing the occurrence of bioclasts replaced by calcite in a microsparite matrix. b) SEM image showing the occurrence of calcareous clay mineralogy and porosity associate to interparticle pores and microchannels. c) SEM image of a microchannel into a calcite matrix, which represents a pathway for gas flow.

petrographic features of the nonlaminated siliceous and fossiliferous claystones are illustrated in Figure 15.

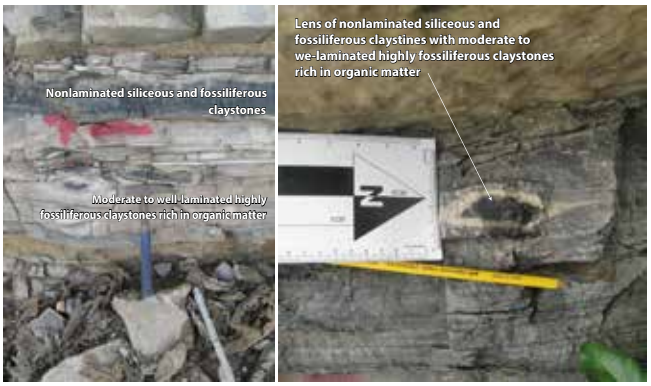

Figure 14. Photographs at outcrop scale of (a)-(b) the nonlaminated siliceous and fossiliferous claystones, developing lenses within moderate to well-laminated highly fossiliferous claystones rich in organic matter.

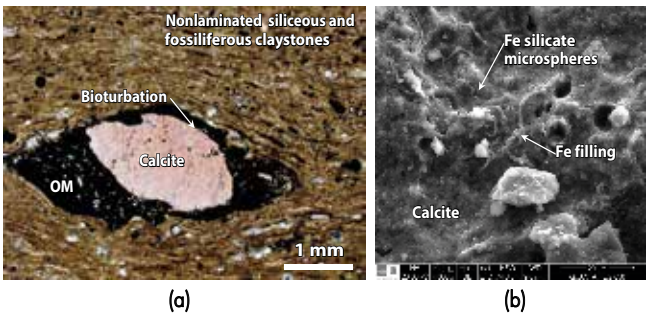

Figure 15. (a) Photomicrograph in crossed polarized light of the nonlaminated siliceous and fossiliferous claystones, showing the occurrence of bioturbation. Note the occurrence of a OM-rich zone around a bioclast. (b) SEM image showing the occurrence of Fe silicate microspheres and Fe filling in a calcite-rich matrix.

Ash falls

This is the least predominant lithofacies in the Aguablanca section (1%), which occurs as very thin layers (up to 2 cm in thickness) in the base, which are rich in kaolinite and silica. It displays a pale yellowish orange color with flecks of very pale orange color that can be attributed to the strong weathering. They are in net contact with highly fossiliferous claystones rich in organic matter. These lithofacies show a long extension and lateral continuity despite its thickness, low hardness compared to the underlying and overlying layers, and easy disintegration (Figure 16). In some layers on the top, it shows higher silica content and in the underlying claystones ripple marks or disturbance of the lamination due to tectonism was observed. It shows a net contact with the underlying claystone layers and gradual transition with the overlying layers. It consists of microcrystalline quartz of tabular habit. The ash falls can be tuffs produced by volcanic eruptions, which expulsed very fine-grained volcanic ash that were airborne, later falling on marine waters and deposited on the bottom. Pyrite (5 wt%), feldspar (4 wt%) and traces of subidiomorphic zircon crystals were observed. The main petrographic features of the ash falls are illustrated in Figure 17.

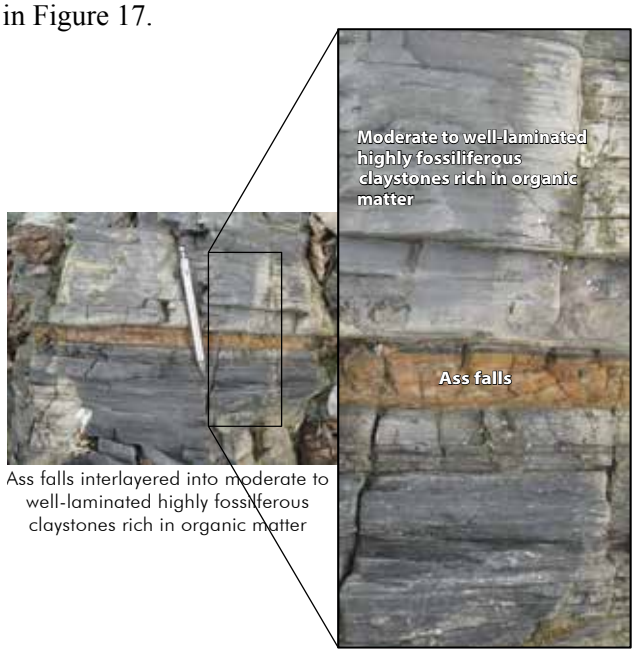

Figure 16. Photographs at outcrop scale of the ash falls, developing very thin layers interbedded into moderate to well-laminated highly fossiliferous claystones rich in organic matter.

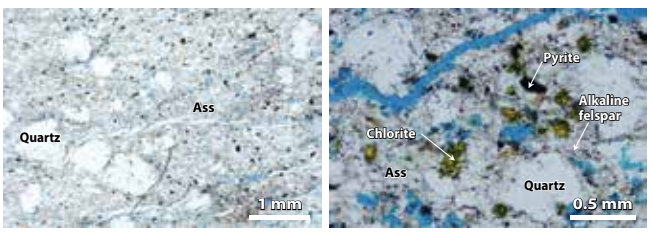

Figure 17. Photomicrographs in cross-polarized light of the ass falls. Note the ocurrence of an ash-rich matrix, where quartz, alkaline feldspar, chlorite and pyrite occur.

7. QUALITY AND MATURITY OF ORGANIC MATTER

Rock Eval data consists of Tmax, oxygen index (OI) and hydrogen index (HI), S1 and S2 values. Geochemical data (Table 1) helped define the thermal maturation level, which can be estimated from the Production Index (PI) obtained from the relationship between the free hydrocarbons (S1), hydrocarbons obtained by primary cracking (S2) and the Tmax value reached during the second stage of pyrolysis, when heavy hydrocarbons produce the peak S2 (McCarthy, Niemann, Palmowski, Peters, & Stankiewicz, 2011). Tmax is the analytical

temperature at which hydrocarbons are released from kerogen and reveal a proxy of thermal maturity (Geel, Schulz, Booth, de Wit, & Horsfield, 2013). According to Geel *et al*. (2013), Tmax values lower than 435 °C indicate immature organic material, between 435 and 455 °C represent mature organic matter and higher than 470 °C are within the gas window. On the other hand, PI values below 0.1 indicate immature organic matter, whereas PI values above 0.4 are within the gas window (Peters, 1986).

The PI vs. Tmax diagram (Figure 18), which helps determining the maturity of the organic matter, shows that most of the Galembo Member rocks have Tmax values ranging from 439 to 448 °C and PI values ranging from 0.02 to 0.1, indicating that these rocks are in the oil window, although with a low PI. The S1 peak corresponds to the free and adsorbed oil, which evaporated at 200-250 °C. The hydrocarbon in these conditions was generated in subsoil but was then expelled during the pyrolysis process. The S2 peak corresponds to the measured potential hydrocarbon that the rock can generate at high temperatures if the maturation of the rock continues. The S3 peak reflects the CO2 and H2O that is released from the thermal cracking of kerogen, during pyrolysis (McCarthy *et al*., 2011). It is important to note that the above list does not take into account the type of organic matter, which other authors (e.g., hilingar, Buryakovsky, Eremenko, & Gorfunkel, 2005) suggest it is important to understand the maturity of organic matter. Furthermore, the result of the PI vs. Tmax was not what waas expected, since although the Tmax is in the oil window, it is maintained in a relatively short range of temperature (439-448 °C) and let to see the relatively constant variation of the PI with respect to depth. The high values of S1 and PI suggest that the primary oil migration occurred in the upper part of the Galembo Member in the section of the Aguablanca Stream and coincides with a Tmax indicating a low thermal maturity in this part of the Galembo Member. At present, two types of diagrams are widely used to interpret the type of organic matter: the HI vs. Tmax and HI vs. OI diagrams (Espitalie *et al*, 1977; Nuñez-Betelu and Baceta, 1994). Both diagrams provide information on the dominant type of kerogen, although the first one also gives an approximate idea of the maturation level. The HI vs. Tmax diagram (Espitalie *et al*, 1977; Gorin and Feist-Bukhardt, 1990) is based on the amount of hydrogen that the kerogen contains and the amount of energy necessary to produce hydrocarbons from that type of kerogen in the laboratory over a short period of time. Espitalié *et al*. (1977) defined the HI

Table 1. Organic geochemical data for the Galembo Member of the La Luna Formation in the Aguablanca section.

Sample	S_1 (mg/g)	S_2 (mg/g)	S_3 (mg/g)	T_{max} (°C)	S_1+S_2 (mg/g)	PI
S- 1 ROO	0.40	3.22	0.22	445	3.620	0.110
S- 2 ROO	0.30	8.46	1.16	444	8.760	0.034
S- 3 ROO	0.48	7.47	0.20	448	7.950	0.060
S- 6 ROO	1.00	8.95	0.32	445	9.950	0.101
S- 7 ROO	0.24	2.52	0.31	445	2.760	0.087
S- 9 ROO	0.00	0.00	0.74	444	0.000	0.000
S-10 ROO	0.19	2.51	0.40	447	2.700	0.070
S-11 ROO	0.07	0.96	1.04	439	1.030	0.068
S-12 ROO	0.75	8.26	0.38	442	9.010	0.083
S-14 ROO	0.11	3.72	1.39	441	3.830	0.029
S-15 ROO	0.05	2.50	0.84	445	2.550	0.020
S-16 ROO	0.16	2.60	0.09	439	2.760	0.058
S-17 ROO	0.80	1.11	0.42	377	1.910	0419
S-18 ROO	0.90	4.01	1.01	442	4.910	0.183
S-19 ROO	0.34	8.71	0.85	442	9.050	0.038
S-20 ROO	0.15	7.65	1.22	441	7.800	0.019
S-21 ROO	0.11	5.92	0.09	445	60.30	0.018
S-22 ROO	0.14	3.10	0.23	446	3.240	0.043

(S2/TOCx100) vs. OI (S3/TOCx100) diagram, which provides valuable information on the type of organic matter, which represents the proportion of hydrogen bound in the organic structure. The HI represents the hydrogen richness and the OI depicts the organic oxygen content of the sample, both relative to the total organic carbon content (Snowdon, 1989). Figure 19 illustrates the relation between HI (mg HC/g TOC) vs. OI (mg CO2/g TOC), with data being plotted on a Van Krevelan diagram, which provides very useful information on the Kerogen type. In general, relatively rapid oscillations in the increase of oxygen and slow periods in the decrease of oxygen in the water column are observed, with a marked increase of oxygen to the top of the Galembo Member, which corresponds to the microfacies of siliceous claystones. Aquatic organic matter has a high HI content whereas terrestrially derived organic matter a low HI, but high OI; the variations of HI values can represent the changing setting of depositional environments (Geel *et al*., 2013). This information is very useful to compare the geochemical and lithostratigraphic characteristics of these rocks, using parameters such as TOC, HI, mineralogy and composition of the matrix determined by petrography, SEM and XRD data. The high values of TOC and HI indicate a good source rock (Ma and Holditch, 2016), with the microfacies of moderate to well-laminated highly fossiliferous claystones rich in organic matter with a matrix composed of clay < 25%, quartz > 35%, which can show the higher fragility. Besides, the TOC values > 2-8 wt%, can define a continue fracture network that promotes the expulsion of bitumen. All the samples are relatively clay-poor, ranging from 6 to 27 wt%, and no apparent trend between TOC values and the total clay contents was observed, being similar to the results reported by Tian *et al*. (2013). The quartz contents vary from 18 to 72 wt% and do not show apparent relationship with TOC (Figure 20). The carbonate contents vary from 18 to 74 wt%. Chalmers, Ross, & Bustin (2012) defined a positive relationship between quartz and TOC contents, which is due to the biogenic origins of quartz. Therefore, taking into account our data and comparing them with those reported by Chalmers *et al*. (2012), the Galembo member rocks contain less quartz of biogenic origin.

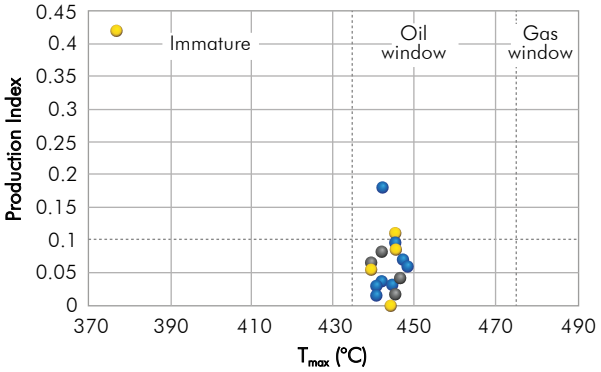

Figure 18. Production Index (PI) vs. Tmax diagram for the Galembo Member of the La Luna Formation in the Aguablanca section.

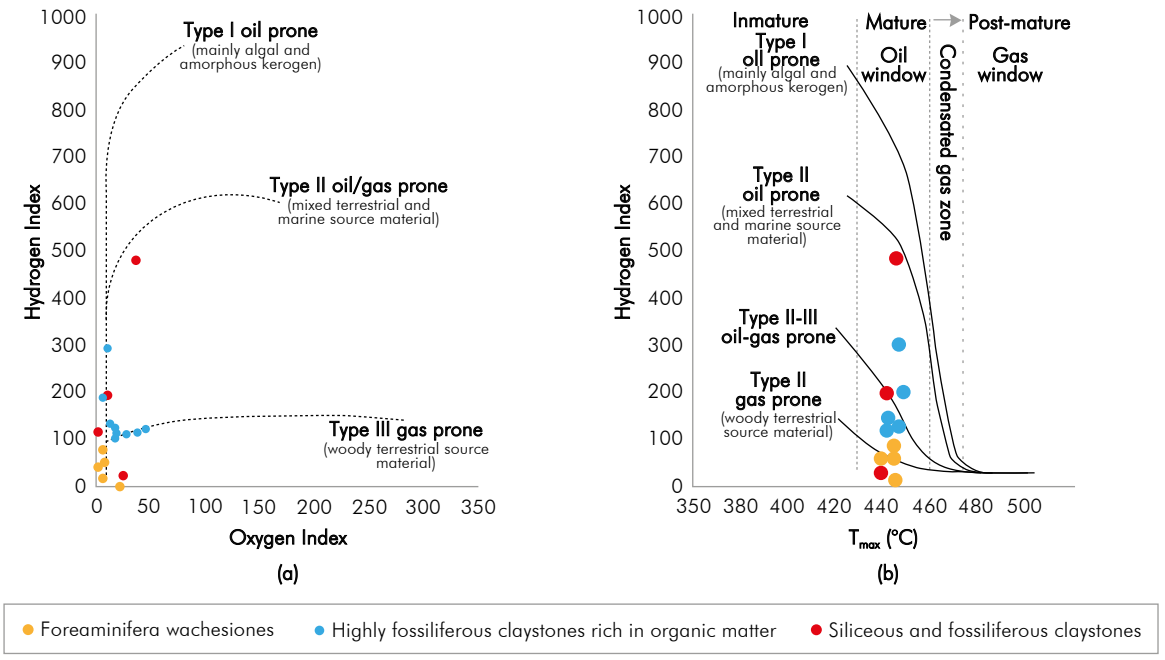

Figure 19. (a) Relationship between HI (mg HC/g TOC) vs. OI (mg CO2/g TOC) and (b) Relation between HI (mg HC/g TOC) vs. Tmax (oC) of shales from the Galembo Member of the La Luna Formation in the Aguablanca section (adapted and modified after Van Krevelan, 1950).

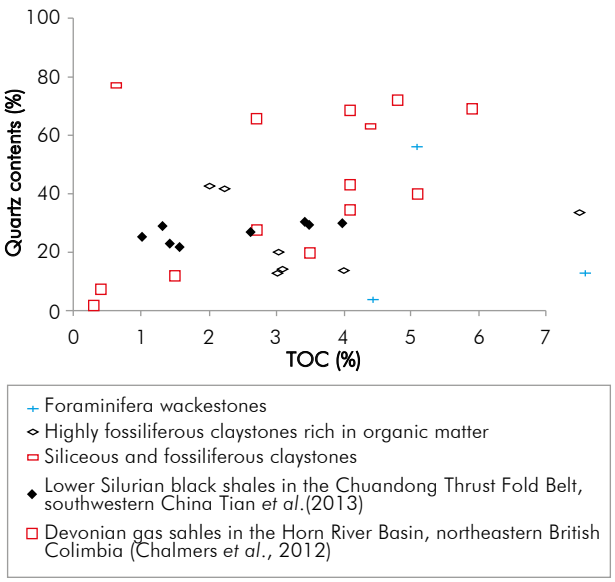

Figure 20. Relationship between quartz contents (%) vs. TOC (%) of the Galembo Member rocks. The reference data are from Devonian gas shales in the Horn River Basin, northeastern British Columbia (Chalmers et al., 2012) and Lower Silurian black shales in the Chuandong Thrust Fold Belt, southwestern China (Tian et al., 2013).

8. DISCUSSION ON THE DEPOSITION MODEL

The observed lithofacies association allowed identifying the depositional environment as a shallow marine, middle to outer shelf, in a transgressing sea. On the basis of sedimentary structures, facies, organic geochemistry, fossil content, and comparisons with regional sedimentological and tectonic features, we propose a model (Figure 21) that accounts for depositional and diagenetic processes and products observed in the Galembo Member of the La Luna Formation. Fossil content show a predominantly deep marine paleoenvironment of deposition. Minor changes can generate variations in the relative proportion of terrigenous material, precipitation of organic matter and diagenetic alterations. Nonlaminated to slight laminated foraminifera wackestones are inferred to have been deposited in deep, still water, where low supply of sediment in areas of low energy hemipelagic sedimentation, which coalesce mainly foraminifera, causing a restriction of these organisms. This is consistent with evidence and models presented by other workers (e.g., Potter, Maynard, & Depetris, 2005) in many analogous settings. The atmosphere is probably in the lower middle part of the foreslope between the underwater slope and basin where conditions change from dysoxic to anoxic. This facies occurs mainly toward the bottom of the Aguablanca section. The microsparite matrix indicates a diagenetic alteration possibly by conversion of carbonate mud (micrite) after the deposition and at the beginning of shallow burial. The foraminiferal wackestone occurs in areas rich in carbonate and poor in organic matter. It presents parallel or subparallel to lamination formed in chemical compaction intermediate burial and hydrocarbon generation window stylolites. Moderate to well-laminated highly fossiliferous laystones rich in organic matter and nonlaminated siliceous and fossiliferous claystones preferably present in anoxic conditions with laminations parallel product underwater currents flow also low input carbonate but high organic matter. The depositional environment is in an underwater basin in areas of low energy where pelagic organisms are deposited. The fine-grained sandy loam are mainly planktonic foraminifera (Globigineroides and Globigirined) and trace content benthic (Textularia), spicules echinoderms, fish bones and fragments of gastropods (broken) possibly carried by submarines flows of low density. A slight increase in the content of benthic foraminifera to the top of the section (0-2%) is observed. The dark gray moderate to well-laminated highly fossiliferous claystones rich in organic matter is mainly comprised of clay-sized particles, which is part of the foraminifera observed in an enlarged upper section (greater foraminifera proportion of coarse sand size towards the middle part of the section). Clay is common to the top of the section long with abundant amounts of quartz mineralogy (13-42 wt%), the increase in the abundance of silica may be caused as a result of the authigenic quartz matrix and deposited in appearance of silica spicules. Calcareous bioclast content is decreasing from the base (3-8%) to stop (3%). The siliceous mineralogy (63-77 wt%) is observed in the matrix of nonlaminated siliceous and fossiliferous claystones; possibly the silica is of volcanoclastic origin, short product flows fall ash mixed with the deposition of the seabed. Excess silica matrix replacing some planktonic foraminifera with microcrystalline quartz or chalcedony. The occurrence of pyrite and organic matter is predominantly toward the top of the section, which is observed by filling fractures, bioclastic and foraminifera. Compaction also increases as the clay mineralogy does. Deformation generated in the concretions of claystones with fossiliferous carbonate concretions with pyrite is due to the early diagenesis, and as concretions are formed adjacent layers begin to deform. Lamination interleaving foraminifera clays reveal this deformation. Two units share the description of the stratigraphic column of the Aguablanca section where changes are shown in the deposition resulting from the extension of the rift during Coniaciano-Santoniano (e.g., Royero and Clavijo, 2001; Potter *et al*., 2005). Therefore, the high

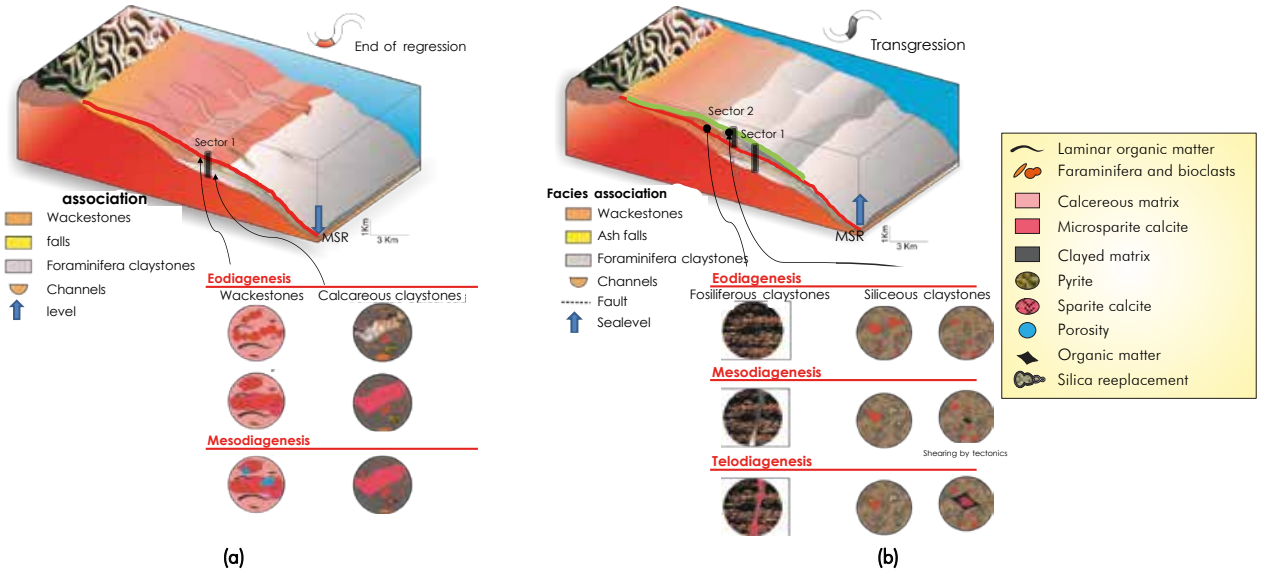

Figure 21. Sketches of the spatial distribution of the deposition sequence and diagenetic variations in the a) Lower and b) Upper units of the Galembo Member (La Luna Formation). MRS: Maximun Regression Surface (red line).

content of organic matter allows us to infer that this corresponds to a high sea level, while the low organic matter content corresponds to a fall in sea level (Torres, 2013). The Aguablanca section displays a relative fall in sea level in the lower unit and then a gradual rise in the upper unit. It can be inferred that these changes in sea level are due to the combination of eustacia and tectonic (Royero and Clavijo, 2001). The change in thickness of the layers, the way the stacked facies, lithologic variations, changes in the types of bioclastic, besides the organic matter content above, leads to propose systemic changes in the depositional environment and stratigraphic sequence.

Lower Unit

The lower unit of the Aguablanca section was placed in a normal regression in an acceleration of the rise in the base level (Catuneanu, 2006; Torres, 2013). The sequence of layers in the Lower Unit shows a slight aggradational stacking in a regressive system. Wackestone facies variation of calcareous claystones in thin layers thick represents a progradation in an atmosphere of deep water. At the height 0-10 m of stratigraphic column bottom to top a small decrease in sea level where the following features are present: concentration of bioclastic and broken gastropods, the highest foraminifera content and a low phosphate concentration. The supply of sediment by underwater currents reflected in the canals of erosive base could cause a relative fall of the sea level and maximum regression surface (MSR). The continuous aggradation and moderate frequency of the layers are responding to turbidity currents generated by eustatic changes in relative variations of sea level with the presence of channels stripping clumps gastropods, bivalves and not differentiated bioclastic. In addition this range of 10-15 m base but increases the size of the layers of calcareous claystones and causes a progressive reduction of the middle layers of wackestone-packestone which suggests an acceleration of the observed baseline level rise (Figure 21a). The observed fossils are broken and disjointed, without preferential orientation, with poor selection. It is inferred that they were transported by debris flows, by continuous aggradation accompanied by tectonic events that accompanied the Upper Cretaceous.

Upper unit

The upper unit is represented by a transgression event. At the top, the sequence changes from moderate to well-laminated highly fossiliferous claystones rich in organic matter facies to nonlaminated siliceous and fossiliferous claystones facies. This unit can be related to a low sedimentation period linked to a sea level rise, allowing an organic matter and phosphates concentration. There is increasing organic matter content and decreased calcareous mineralogy; it follows that corresponds to the increase in sea level. This unit presents a thickening upward pattern with absence of erosive channels in the layer contact plane and an upward increasing concentration of organic matter and in contrast an upward decreasing of carbonate minerals. The sea level rise may be due to the combination of eustasy and subsidence associated with the extension of rift during the Coniacian-Santonian (Figure 21b).

The depositional environment of the Upper Unit was affected by changes in the rising sea level where changes in circulation and intensities of nutrients are evident, inducing decreasing oxygenation and a decrease of the amount of planktonic foraminifera planktonic and bioclastic, as can be observed in this study.

4. CONCLUSIONS

- The integration of different stratigraphic and mineralogical data for lithofacies analysis let to recognize five general lithofacies in the Aguablanca section: (1) nonlaminated to slight laminated foraminifera wackestones, (2) moderate to well-laminated highly fossiliferous claystones rich in organic matter; (3) claystones with fossiliferous carbonate concretions with pyrite; (4) nonlaminated siliceous and fossiliferous claystones; (5) ash falls. It was concluded that the grains that make up the lithofacies of the Aguablanca section are intrabasin (foraminifera, undifferentiated bioclastic limestone matrix, etc.) and extrabasin (ash fall, detrital quartz, etc.). Moderate to well-laminated highly fossiliferous claystones rich in organic matter and nonlaminated siliceous and fossiliferous claystones with higher content of quartz and calcite can be considered as the most suitable zones to be fracked. Data collected and analyzed helped distinguish two units in the Aguablanca section. Changes in the limestone and clay mineralogy have a lateral and vertical variation. Most clay content and mineralogy quartz is in the Upper Unit of the section. This unit presents a decrease of calcareous minerals and sometimes the content of foraminifera. The energy deposition time is variable. The Lower Unit shows a high energy by the appearance of erosive channels and rip-up structures. Energy of the Superior Unit is lower due to the absence of submarine channels and contact planar layers. The eustasy and changing ocean conditions are the dominant factor in the deposition of the Aguablanca section. All these features allow to infer that the lower unit could be deposited at the end of a typical marine regression MSR, while the upper unit has a typical stack of TST. From a diagenetic point of view, it is possible to relate the stratigraphic sequence with the deposition and the subsequent diagenetic change of the rock. Comparing the results obtained in this study with those reported by several authors (e.g., Morales, 1958; Rangel *et al*., 2000a, 2000b; Torres, 2013) it can be concluded that the Pujamana Member proposed by other authors corresponds to the Galembo Member in the Aguablanca section, based on petrographic and geochemical characteristics. It is suggested that the heavy minerals in the tuffs found along the Aguablanca Section, along with ammonites and foraminifera to date the rock and strengthen the age of exposed rock section.

ACKNOWLEDGEMENTS

This work was part of the MSc Thesis carried out by Efrain Casadiego at the Universidad Industrial de Santander, Colombia. The authors thank to the Universidad Industrial de Santander through its laboratories of Transmitted Light Microscopy of the Research Group in Basic and Applied Geology and the Geochemistry of the Research Group in Hydrocarbon Geology, as well as the X-Ray and Microscopy laboratories of the Central Laboratory (Guatiguará Technological Park) and their professional staff for their assistance with XRD and SEM data acquisition and analyses. We are also in huge debt with anonymous reviewers for their helpful comments and suggestions to this manuscript. The authors are very grateful to the above-named people and institutions for their support.

REFERENCES

Abdel-Rahman, A.Y.A. (2013). Thermal maturity and hydrocarbon potential of jurassic sediments, Northeastern Sinai, Egypt. *Middle-East J. Sci. Res*., 18(2), 183-190.

Aguilera, R.C., Sotelo, V.A., Burgos, C.A., Arce, C., Gómez, C., Mojica, J., Castillo, H., Jiménez, D. & Osorno, J. (2009). Organic geochemistry atlas of Colombia: An exploration tool for mature and frontier basins. *Earth Sci. Res. J*., 13, Special Edition, 1-174.

Agencia Nacional de Hidrocarburos (ANH) (2008). Colombian Sedimentary Basins: Nomenclature, boundaries and petroleum geology, a new proposal, 92p.

Arthur, M. A., Schlanger, S.O. & Jenkyns, H.C. (1987). The Cenomanian-Turonian oceanic anoxic event II, paleoceanographic controls on organic matter production and preservation. In: Brooks, J. & Fleet, A. (Eds) Marine Petroleum Source Rocks. Geol. *Soc. Spec. Publ*. 24, pp. 399– 418.

Ballesteros, C.A. & Parra J.A. (2012). Estudio estratigráfico secuencial para la Formación La Luna en el costado

oriental de la Cuenca del Valle Medo del Magdalena: Una visión exploratoria de hidrocarburos no convencionales. Undergraduate Thesis, Universidad Industrial de Santander, Bucaramanga, Colombia. 112p.

Bersezio, R., Erba, E., Gorza, M. & Riva, A. (2002). Berriasian–Aptian black shales of the Maiolica Formation (Lombardian Basin, Southern Alps, Northern Italy): local to global events. *Palaeogeogr. Palaeoclimatol. Palaeoecol*., 180, 253-275.

Bralower, T.J. & Lorente, M.A. (2003). Paleogeography and Stratigraphy of the La Luna Formation and Related Cretaceous Anoxic Depositional Systems. *Palaios,* 18, 301-304.

Casadiego, E. (2014). Caracterización de reservorios de gas shale integrando datos multiescala: Caso estudio Miembro Galembo, Sección Aguablanca, Cuenca del Valle Medio del Magdalena. Undergraduate Thesis, Universidad Industrial de Santander, Bucaramanga, Colombia.

Catuneanu, O. (2006). Principles of Sequence Stratigraphy. Elsevier, Amsterdam, 375p.

Chalmers, G.R.L., Ross, D.J.K. & Bustin, R.M. (2012). Geological controls on matrix permeability of Devonian Gas Shales in the Horn River and Liard basins, northeastern British Columbia, Canada. *Int. J. Coal Geol*. 103, 120-131.

Chilingar, G.V., Buryakovsky, L.A., Eremenko, N.A. & Gorfunkel, M.V. (2005). Geology and Geochemistry of Oil and Gas, Elsevier Science & Technology, 390p.

Dunham, R.J. (1962). Classification of Carbonate Rocks According to Depositional Texture. In: Hamm, W.E. (Eds.), Classification of Carbonate Rocks, AAPG Memoir 1, 108-121.

Erbacher, J., Huber, B.T., Norris, R.D. & Markey, M. (2001). Increased thermohaline stratification as a possible cause for an ocean anoxic event in the Cretaceous period. *Nature* 409, 325-327.

Espilalié, J., Laporte, J.L., Madec, M., Marquis, F., Leplant, P. & Paulet, J. (1977). Méthode rapide de characterisation des roches mères, de leur potentiel petrolier et de leur degré d'évolution. *Revue I. Fr. Pétrol*. 32(1), 23-45.

Espitalié, J., Deroo, G. & Marquis, F. (1986). La pyrolyse Rock–Eval et ses applications. *Revue I. Fr. Pétrol.,* 41, 73–89.

Folk, R.L. (1974). Petrology of Sedimentary Rocks. Hemphill Publishing Company, Austin, 182p.

Garner, A.H. (1926). Suggested nomenclature and correlation of the geological formations in Venezuela. *Am. I. Min. Metall. Eng. Trans.,* 1, 677-684.

Geel, C., Schulz, H.-M., Booth, P., de Wit, M. & Horsfield, B. (2013). Shale gas characteristics of Permian black shales in South Africa: results from recent drilling in the Ecca Group (Eastern Cape). *Energy Procedia,* 40, 256-265.

Gorin, G.E. & Feist-Bukhardt, S. (1990). Organic facies of Lower to Middle Jurassic sediments in the Jura Mountains, Switzerland. *Rev. Paleobot. Palyno*., 65, 349-355.

Govea, C. and Aguilera, H. (1985). Cuencas sedimentarias de Colombia. II Simposio Bolivariano - Exploración en Cuencas Subandinas, Bogotá, 93p.

Hedberg, H.D. & Sass, L.C. (1937). Synopsis de las formaciones geológicas de la parte occidental de la Cuenca de Maracaibo, Venezuela. Servicio Técnico de Geología y Minería, Caracas, Boletín de Geología y Mineralogía (Venezuela), 2-4, 83–84.

Hubach, E. (1957). Estratigrafía de la Sabana de Bogotá y alrededores. Instituto Geológico Nacional, Boletín Geológico 5(2), 93-112.

Ingersoll, R.V., Bullard, T.F., Ford, R.L., Grimm, J.P., Pickle, J.D. & Sares, S.W. (1984). The effect of grain size on detrital modes: A test of the Gazzi-Dickinson point-counting method. *J. Sediment. Petrol.,* 54, 103–116.

Juliao, T., Suárez-Ruiz, I., Marquez, R. & Ruiz, B. (2015). The role of solid bitumen in the development of porosity in shale oil reservoir rocks of the Upper Cretaceous in Colombia. *Int. J. Coal Geol*., 147–148, 126-144.

Kretz, R. (1983). Symbols for rock-forming minerals. *Am. Mineral.,* 68, 277-279.

Law, B.E. & Curtis, J.B. (2002). Introduction to unconventional petroleum systems. *AAPG Bull.,* 86(11). 1851–1852.

Ma, Y.Z. & Holditch, S.A. (2016). Unconventional Oil and Gas Resources Handbook: Evaluation and Development. Elsevier, USA. 84pp.

Mann, U. & Stein, R. (1997). Organic facies variations, source rock potential, and sea level changes in Cretaceous black

shales of the Quebrada Ocal, Upper Magdalena Valley, Colombia. *AAPG Bul.,* 81(4), 556–576.

McCarthy, K., Niemann, M., Palmowski, D., Peters, K. & Stankiewicz, C. (2011). La geoquímica básica del petróleo para la evaluación de las rocas generadoras: *Oilfield Rev*., 23 (2), 35-47.

Montgomery, S. (1992). Petroleum potential of Upper and Middle Magdalena basins, Colombia. *Petrol. Frontiers,* 9(3), 67p.

Morales, L.G., Podesta, D.J., Hatfield, W.C., Tanner, H., Jones, S.H., Barker, M.H., O'Donoghue, D.J., Mohler, C.E., Dubois, E.P., Jacobs, C. & Goss, C.R. (1958). General Geology and oil occurrences of the Middle Magdalena Valley, Colombia. In: Weeks, L.G. (Eds.), Habitat of Oil Symposium. *AAPG 41*, 641-695.

Nuñez-Betelu, L, & Baceta J.I., (1994). Basics and Application of Rock-Eval/TOC Pyrolysis: an example from the uppermost Paleocene/lowermost Eocene in the Basque Basin, Western Pyrenees. *Natur Zientziak* 46, 43-62.

Maughan, E.K., Zambrano, F., Mojica, P., Abozaglo, J., Pachon, F. & Duran, R. (1979). Paleontologic and stratigraphic relations of phosphate beds in Upper Cretaceous rocks of the Cordillera Oriental, Colombia. U.S. Geological Survey, 101p.

Mayorga, L.A. & Piamonte, D.A. (2015). Caracterización de yacimientos tipo Shale Gas y Oíl Shale de la Formación La Luna en el flanco Oriental de la Cuenca del Valle Medio del Magdalena (VMM), Santander, Colombia. Tesis de Pregrado, Universidad Industrial de Santander, Bucaramanga, Colombia.

Naranjo, V., Duque, N. & Moreno, N. (2009). Definición de eventos diagenéticos y carga de hidrocarburos mediante estudios de petrología en La Formación Rosablanca, Cuenca del Valle Medio del Magdalena. 10th Simposio Bolivariano - Exploracion Petrolera en las Cuencas Subandinas. Resumen. ACGGP.

Pacheco-Sintura, P.A., Cardona-Molina, A. & Cortés, F.B. (2015). Compositional characterization and storage capacity of shale samples from La Luna and Conejo Formations (Middle Magdalena basin and the Eastern Cordillera): Implications for evaluation of cretaceous shale gas in Colombia. *Bol. Cie. Tierra,* 37, 45-53.

Perez-Tellez, G. (1994). The La Luna petroleum system of Colombia. Fisrt Jt, AAPG/AMPG Research Conference, 5pp.

Peters, K.E. (1986). Guidelines for evaluating petroleum source rock using programmed pyrolysis. *AAPG Bulletin,* 70(3), 318-329.

Potter, P.E., Maynard, J.B. & Depetris, J.P. (2005). Mud and Mudstones. Springer-Verlag, Germany., 297pp.

Poulsen, Ch.J., Barron, E.J., Arthur, M.A. & Peterson, W.H. (2001). Response of the mid-Cretaceous global oceanic circulation to tectonic and CO2 forcings. *Paleoceanogr.,* 16(6), 576-592.

Rangel, A., Giraldo, B., Magoon, L., Sarmiento, L.F., Bartels, H., Mora, C., Cordoba, F., Luna, O. & Reyes, J.P. (1996). Oil potential of the Cretacic megasequence and associated oil families in the Middle Magdalena Valley, Colombia. Memorias del V Congreso Latinoamericano de Geoquímica Orgánica, Cancún, 105pp.

Rangel, A., Giraldo, B., Munar, R., Olaya, I., García, M., Gutierrez, J., Parra, P. & Niño, Ch. (2000a). Estratigrafía química y facies orgánicas del Terciario Inferior y Cretácico Superior del Piedemonte Llanero y Valle Oriental del Magdalena. Internal Report ECOPETROL- ICP.

Rangel, A., Parra, P. & Niño, C. (2000b). The La Luna Formation: chemostratigraphy and organic facies in the Middle Magdalena Basin. *Org. Geochem*. 31(12), 1267-1284.

Ramon, J.C. & Dzou, L.I. (1999). Petroleum geochemistry of the Middle Magadalena Valley: Colombia. *Org. Geochem*., 30(4), 249-266.

Rey, O., Simo, J.A & Lorente, M.A. (2004). A record of long- and short-term environmental and climatic change during OAE3: La Luna Formation, Late Cretaceous (Santonian–early Campanian), Venezuela. *Sediment. Geol.,* 170 (1–2), 85-105.

Rodriguez, J.C. (2013). Challenges and opportunities for the development of Shale resources in Colombia. MSc thesis, The University of Texas, Austin.

Ross, D.J.K. & Bustin, R.M. (2008). Characterizing the shale gas resource potential of Devonian–Mississippian strata in the Western Canada sedimentary basin: Application of

an integrated formation evaluation. AAPG Bulletin, 92(1), 87–125.

Royero, J. & Clavijo, J. (2001). Mapa Geológico generalizado departamento de Santander. Escala 1: 400.000. Informe INGEOMINAS, 92pp.

Russell, D.A. & Paesler, M.A. (2003). Environments of Mid-Cretaceous Saharan dinosaurs. *Cretaceous Res*., 24(5), 569-588.

Schamel, S. (1991). Middle and Upper Magdalena Basins, Colombia. In: Biddle, K.T. (Eds.), Active Margin Basins. *AAPG Memoir,* 52, 283-301.

Schieber, J., Southard, J. & Thaisen, K. (2007). Accretion of Mudstone Beds from Migrating Floccule Ripples. *Science*, 318 (5857), 1760-1763.

Slatt, R.M. (2011). Important Geological Properties of Unconventional Resource Shales. *Cent. Eur. J. Geosci.,* 3, 435-448.

Snowdon, L.R. (1989). Organic matter properties and thermal evolution. In: Short course in burial diagenesis. Hutcheon, I.E. (Eds.). Mineralogical Association of Canada, Short Course Handbook, 15, 39-40.

Sorkhabi, R. (2009). The Mid-Cretaceous Source Rock Enigma. *Geo Expro,* 6(5), 24-30.

Talukdar, S., Gallango, O. & Ruggiero, A. (1985). Formaciones La Luna y Querecual: rocas madres de petróleo. En: Espejo, A., Ríos, J.H., De Bellizzia, N.P., De Pardo, A.S. (Eds.), Memoria: VI Congreso Geológico Venezolano, Memorias. Sociedad Venezolana de Geológos, Caracas, 3606–3642.

Tian, H., Pan, L., Xiao, X., Wilkins, R.W.T., Meng, Z. & Huang, B. (2013). A preliminary study on the pore characterization of Lower Silurian black shales in the Chuandong Thrust Fold Belt, southwestern China using low pressure N2 adsorption and FE-SEM methods. *Mar. Petrol. Geol.,* 48, 8-19.

Torres, E.J. (2013). Unconventional gas shale assessment of La Luna Formation in the central and south areas of the Middle Magdalena Valley Basin, Colombia. MSc thesis. University of Oklahoma, Norman.

Torres, E.J., Slatt, R.M., Philp, P., O´Brien, N.R. & Rodriguez, H.L. (2012). Characterization of the Cretaceous La Luna Formation as a shale gas system, Middle Magdalena Basin, Colombia. Houston Geological Society. Poster.

Torres, E.J., Slatt, R.M., Philp, P., O´Brien, N.R. & Rodriguez, H.L. (2015). Unconventional Resources Assessment of La Luna Formation in the Middle Magdalena Valley Basin, Colombia. AAPG Annual Convention & Exhibition, Denver, Colorado, 2015.

Villamil, T. (1999), Campanian-Miocene tectonostratigraphy, depocenter evolution and basin development of Colombia and western Venezuela. *Paleogeogr. Paleoclimatol. Paleoecol.,* 153, 239-275.

Young, A., Monaghan, P.H. & Schweisberger, R.T. (1977). Calculation of ages of hydrocarbons in oils - Physical chemistry applied to petroleum geochemistry I. *AAPG Bulletin,* 61(4), 573-600.

Zumberge, J.E. (1980). Oil-oil and oil-source rock correlations of bacterially degraded oils and Cretaceous outcrops from Colombia, South America (Abstract). Paris, International Geological Congress, 26, p. 806.

Zumberge, J.E. (1984). Source Rocks of the La Luna Formation (Upper Cretaceous) in the Middle Magdalena Valley, Colombia. In: Palacas J. (Eds.), Petroleum Geochemistry and Source Rock Potential of Carbonate Rocks. *AAPG Studies in Geology,* 18, 127-133.

AUTHORS

Efrain Casadiego-Quintero
Affiliation: *Universidad Industrial de Santander*
e-mail: ecasageo@gmail.com

Carlos Alberto Ríos Reyes
Affiliation: *Universidad Industrial de Santander*
e-mail: carios@uis.edu.co